Multiple-Hole Effect on the Performance of a Sparger During Direct Contact Condensation of Steam

Seok Cho[*†], **Chul-Hwa Song, Heung-June Chung, Se-Young Chun, Moon-Ki Chung**
Korea Atomatic Energy Research Institute

An experimental study has been carried out to investigate an I-type sparger performance in view of pressure oscillation and thermal mixing in a pool. Its pitch-to-hole diameter, P/D, varies from 2 to 5. The test conditions are restricted to the condensation oscillation regime. In the present study, two different hole patterns, staggered and parallel types, are employed under various test conditions. The amplitude of the pressure pulse shows a peak for pool temperatures of 45~85℃, which depends on P/D and the steam mass flux. The effect of hole pattern on the pressure load is smaller than that of *P/D*. The dominant frequency increases with the subcooling temperature of pool water and P/D. A correlation for the dominant frequency is proposed in terms of the pitch-to-hole diameter ratio and other dimensionless thermal hydraulic parameters.

Key Words : Sparger, Pressure Load, Thermal Mixing, Pitch-to-Hole Diameter Ratio

Nomenclature ————————————

a	: Exponent
b	: Exponent
c	: Exponent
C_p	: Specific heat, kJ/kg°K
d	: Exponent
D	: Hole diameter, m
f	: Frequency, Hz
G	: Steam mass flux, kg/m²-s
h_{fg}	: Latent heat, kJ/kg
I_{ϕ}	: Shape factor of sparger
Ja	: Jacob number, $\rho_l C_{pl} \Delta T / \rho_s h_{fg}$
k	: Constant
P	: Pitch or Pressure, m or kPa
Re	: Reynolds number, $\rho_s VD/\mu$
St	: Strouhal number, $fD\rho_l/\rho_s V$
T	: Temperature, ℃
T_m	: Mean temperature ℃
T_{sat}	: Saturation temperature, ℃

ΔT	: Pool subcooling, ℃
V	: Velocity, m/s
We	: Weber number, $\rho_s V^2 D/\rho$

Greek Symbols

ρ	: Density, kg/m³
μ	: Viscosity, N-s/m²
σ	: Surface tension of water at steam temperature, N/m

Subscripts

a	: Atmospheric condition
l	: Liquid
m	: Mean value of pool water
s	: Steam

† First Author
* Corresponding Author,
  E-mail : scho@kaeri.re.kr
  TEL : +82-42-868-2719; **FAX :** +82-42-868-8362
  Korea Atomic Energy Research Institute, 150 Dukjin-dong, Yusong-ku, Taejon 305-353, Korea.(Manuscript
  Received June 15, 2000; **Revised** December 27, 2001)

1. Introduction

Direct contact condensation (DCC) phenomena is encountered in several components of a nuclear power plant during transient, or accident conditions. For example, in the loss of coolant accident (LOCA) of a pressurized water reactor, steam may come into direct contact with cold

water at several locations such as a cold leg, a downcomer, a hot leg, and upper and lower plena. DCC phenomena are also expected to occur in the in-containment refueling water storage tank (IRWST) of the Korea Next Generation Reactor (KNGR), when the reactor depressurization system valves or the pressurizer safety valves are open to discharge steam into the quench tank through a steam discharge device (sparger). Understanding the DCC phenomena is important for optimal sparger design to ensure structural integrity of the reactor system and their safe operation.

Although many studies on the DCC phenomena exist, the phenomena are not yet well understood. The previous works were mainly focused on correlating heat transfer coefficient and dimensionless jet length with steam mass flux and pool water temperature. Moreover, all the previous works employed a single-hole nozzle. According to Arinobu (1980) the dominant frequency of the pressure pulse decreases with increasing pool temperature and nozzle diameter, but increases with increasing steam mass flux. Based on experimental observations, he proposed the frequency relation in Eq. (1).

$$f = 0.8 V/D [(C_P \Delta T)/h_{fg}]^{1.4} \qquad (1)$$

where f is the dominant frequency in Hz and V is the steam velocity at the exit of the vent pipe in m/s. Fukuda (1982) also asserted that the dominant frequency is proportional to the degree of pool water subcooling and inversely proportional to the nozzle size. He suggested the simple frequency relation as follows:

$$f = 60.0 \Delta T/D \qquad (2)$$

where ΔT is the subcooling temperature of water in ℃. Cho et al. (1999) suggested that in some operating conditions, condensation takes place in a very unstable manner so that the steam jet begins to oscillate with large pressure pulses. They emphasized that the transition between unstable and stable regimes depends on the nozzle diameter, the steam mass flux, and the pool water temperature.

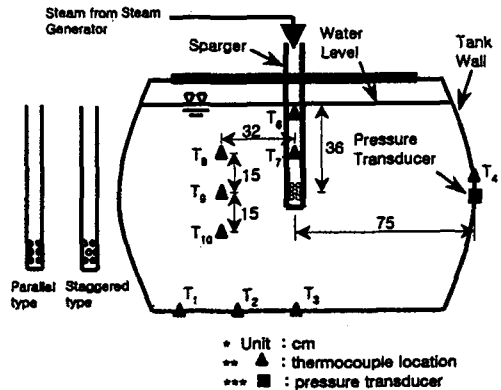The previous works mentioned above simply

Fig. 1 Schematic diagram of the sparger and the locations of the instrumentation in the pool

presented the characteristics of a single-hole nozzle (or vent tube). Sparger, however, is a multi-hole device. The pressure pulse characteristics of a multi-hole sparger is expected to be different from those of a single-hole nozzle due to the interaction of the discharging steam jets. To expand the single-hole relations to a multi-hole sparger, the interaction of the discharging steam with its neighboring steam jets and the sparger shape factor, which can be represented by the pitch-to-diameter ratio, P/D, and the hole distribution pattern must be considered.

The overall objective of the present study is to provide the basic understanding of the conden-ation characteristics of the multi-hole sparger. First objective is to investigate the dynamics of pressure oscillations in terms of amplitude and dominant frequency when steam is fed through various kinds of multi-hole I-type spargers in subcooled water. Second objective is to investigate the performance of each sparger tested here with respect to the pressure behavior and thermal mixing effect in a pool. Third objective is to compare multi-hole sparger data with those of a single-hole nozzle to clarify the multi-hole effect. These data will enrich the database on the performance of several types of spargers.

2. Experimental Method

The experimental facility consists of a steam generator, a quenching tank, steam supply lines,

Table 1   Test conditions and technical specifications of the sparger

Sparger Type	Sp1	Sp2	Sp3	Sp4	Sp5	Sp6	Sp7	Sp8
Pattern of hole (S : staggered, P : parallel)	S	P	S	P	S	P	S	P
Total number of holes (EA)	20		21		20		20	
P/D ratio	2		3		4		5	
Hole diameter (mm)	5							
Nominal size of sparger (mm)	1 inch, Schedule 40, ANSI stainless pipe							
Total hole area /Flow area of sparger (%)	70.7		74.2		70.7		70.7	
Steam mass flux (kg/m²-s)	70~215							
Pool temperature (℃)	30~95							

valves and instruments. A schematic diagram showing the sparger and the locations of the instruments in the quench tank is shown in Fig. 1. The steam generator with 300 kW electric heaters continuously produced steam with dryness higher than 99%. The maximum operating pressure was 1.03MPa and the maximum steam flow rate was 0.12kg/s. Subcooled water is contained in the quenching tank equipped with two plexi-glass windows for visual observation and video camera imaging. The quenching tank is a horizontal cylindrical tank open to atmosphere, with a diameter of lm and length of 1.5m. The nominal size of the steam supply line is 1 inch, Schedule 40, ANSI standard stainless pipe. The steam supply line is heated by trace heaters and insulated in order to maintain the supplied steam saturated with about 99% dryness during the test. A vortex type steam flow meter, a manual flow control valve, a drain valve, an isolation valve, a pressure transmitter, and a thermocouple are installed in the steam supply line. Nine thermocouples are also installed inside the quenching tank to measure the pool temperature, and a piezoelectric type pressure transducer is installed on the tank wall, 75 cm away from the sparger axis. A data acquisition system, which consists of an IBM-compatible computer and a 12-bit A/D converter, processes all the signals. The sampling rate is 4,096Hz. All of the instruments were calibrated before testing.

Eight different kinds of spargers with a steam-discharging hole diameter of 5 mm were tested for various combinations of steam mass flux and the pool temperature. The manual flow control valve in the steam supply line controls the steam mass flux. The centerline of sparger's vertically distributed injection holes is maintained at about 36 cm below the free surface of the pool water during the test.

When the steam generator isolation valves are opened, a small amount of water and air inside the steam supply line is discharged first. After clearing out the water and air in the line, steam from the steam generator is continuously discharged into the pool. During the initial stage of steam discharge, dissolved gas in the pool form tiny gas bubbles, but they disappear when the pool temperature is above 30 ℃. As steam is continuously discharged into the pool, the mean temperature of subcooled water in the quench tank increases until it reaches a pre-set value. The test conditions and technical specifications of spargers are listed in Table 1.

3. Experimental Results and Discussion

DCC phenomena can be classified mainly in terms of steam mass flux and water subcooling in the condensation flow regime map (Aya et al., 1983; Sonin, 1984). For a steam mass flux lower than 55~65 kg/m²-s, chugging phenomenon may occur (Chan, 1978). For steam mass fluxes higher
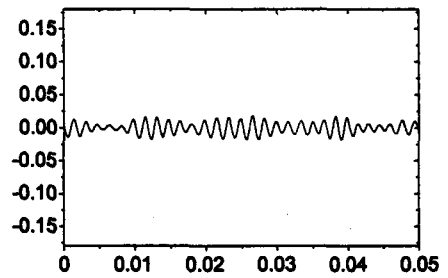
(a) $T_\pi = 35.2°C$

(b) $T_\pi = 65.1°C$
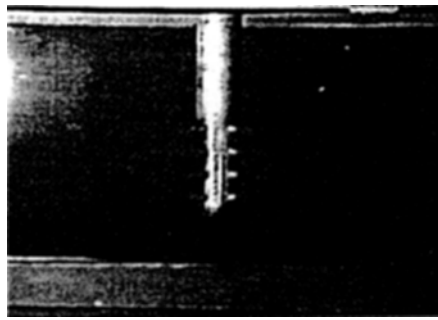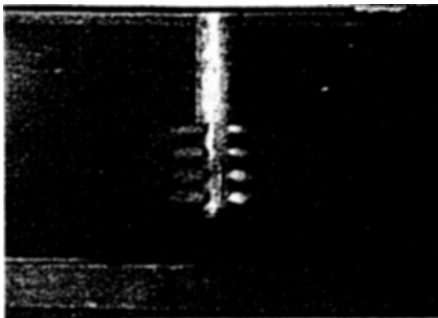
(c) $T_\pi = 94.9°C$

Fig. 2 Typical shapes of the steam jet in the case of Sp6 at $G = 106$ kg/m²-s

(a) $T_\pi = 40.1°C$

(b) $T_\pi = 55.3°C$

(c) $T_\pi = 75.1°C$

(d) $T_\pi = 80.0°C$
Time[sec]

Fig. 3 Pressure signal measured at the wall with a variation of pool temperature in the case of Sp8 at $G = 141$kg/ m²-s

than 70 kg/m²-s, periodic pressure variation induced by oscillatory movement of the steam-water interface is sometimes observed. This phenomenon is called a condensation oscillation. Typical images of steam jets taken for Sp6 at $G = 106$kg/m²-s are shown in Fig. 2. As the pool temperature increases, the steam jets' length & diameter become increase, and the jets combine with neighboring ones.
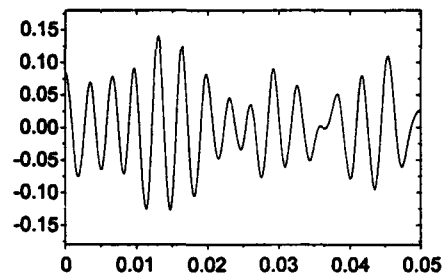
Typical pressure signals observed for Sp8 with a mass flux of 141 kg/m²-s are shown in Fig. 3. The pressure pulse at the low temperature condi-

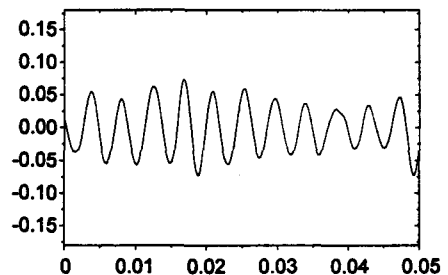tion has a small amplitude and a high frequency. As the pool temperature increases, the amplitude reaches its peak and then it decreases with increasing pool temperature. The frequency of positive peak pressure decreases as the pool temperature increases. Thus, pool temperature strongly influences the amplitude and the frequency of pressure oscillation.

3.1 Amplitude of the pressure pulse

In this section, the influence of steam mass flux and pool temperature on the pressure amplitude is discussed. Figures 4 and 5 show the variation of root-mean-square pressure amplitude versus steam mass flux and pool temperature, for the eight different spargers. According to Cho et al. (1999), the the pressure pulse amplitude is closely related to condensation modes. In other words, the pressure pulses in a condensation oscillation mode show much larger amplitudes than those in a stable condensation mode, when the pool temperature is maintained at a constant level. The difference between the pressure amplitudes of the two condensation modes decreases as the pool temperature increases. Therefore, the test conditions in the present study are limited to the condensation oscillation mode.

In single nozzle experiments (Cumo et al., 1978; Damasio et al., 1985; and Tin et al., 1982), the amplitude of the pressure pulse initially tends to increase with increasing pool temperature. The amplitude reaches a peak value at pool temperatures of between 60 and 80 ℃. Sonin (1984) suggested that the peak may occur at a finite subcooling because the peak amplitude requires a low subcooling to form a large bubble and a high subcooling for a short collapse time. The pressure then decreases steeply before water reaches its saturation temperature. This same trend was observed in the present study (Figs. 4 and 5).

In the present study, however, the pressure peaks appear lower mean temperatures than those in previous works, especially in the cases of low steam mass flux conditions with Sp1 and Sp2. This phenomenon is explained by considering both the interaction of neighboring steam jets and

the difference between the water temperature in the vicinity of steam-water interface and the mean temperature of pool water. The P/D ratio of Sp1 and Sp2 is 2, which is very small. Therefore, the steam jets tend to become more interactive with neighboring jets than those in other spargers. During this interaction, steam jets combine with other jets to build donut-shaped unstable bubbles around the sparger. Consequently, steam jet's kinetic-energy, a driving force for thermal mixing, is decreased rapidly. Thus, the temperature of water in the vicinity of the steam bubble-water interface increases more rapidly than the mean temperature of the pool water due to the weak convective force around the steam jets. The condensation dynamics is affected not by the mean temperature of subcooled water, but by the local temperature around the steam-water interface.

Considering the descriptions mentioned above, it could be quite well understood the reason why the peaks occur at a relatively low mean temperature of pool water with Sp1 and Sp2. The dynamics of the DCC of steam discharging through a multi-hole sparger are partially affected by the interaction of neighboring steam jets. However, the interaction is also closely related to the sparger, configuration such as the P/D ratio. As P/D decreases, the interaction effects intensity. Therefore, to characterize the dynamics of DCC through a multi-hole sparger, the hole configuration effects must be considered.

Figures 4 and 5 show that the pressure peaks at a specified steam mass flux are occur for pool temperatures between 45~85 ℃, and the peak pressure temperature increases with steam mass flux. Also, the peak amplitudes increase with P/D. However, the amplitudes of staggered-type spargers are nearly equivalent to those of parallel-type spargers. Thus, the hole distribution pattern is less important than P/D.

Figure 6 shows the difference between the pool water mean temperature and the local temperature, T_3, at the bottom of the tank (Fig. 1), at a steam mass flux of 71 kg/m²-s. The mean temperature is obtained with three different thermocouples located in the quench tank (thermocouples-7, 8, and 10 in Fig. 1). Therefore,
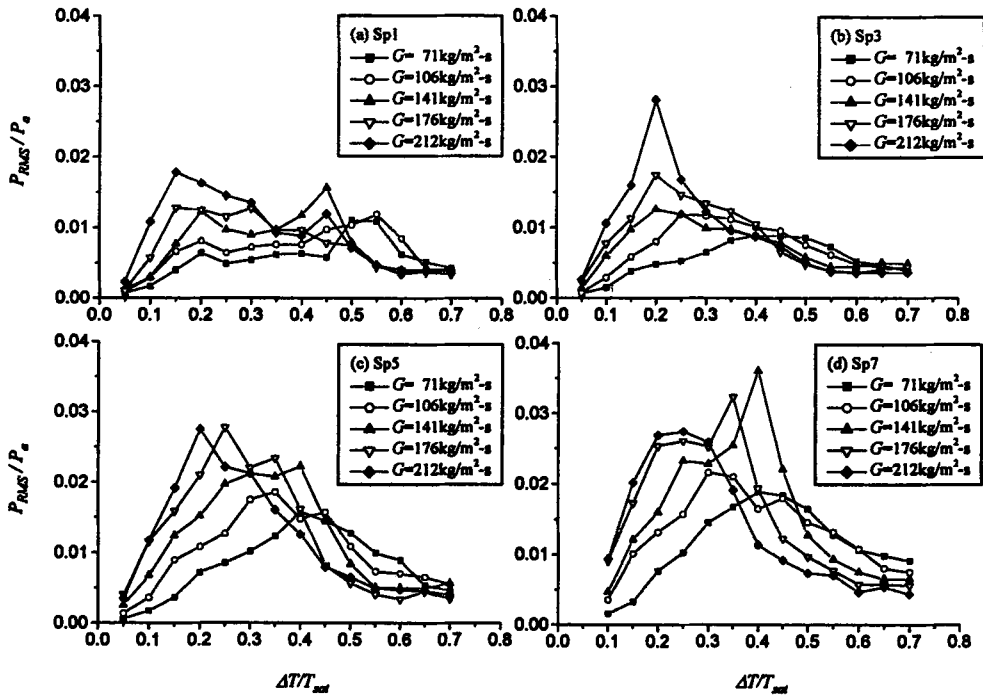
Fig. 4   Variation of pressure amplitude of staggered type spargers

the temperature difference serves as a potential indicator of the thermal mixing performance of each sparger. A larger temperature difference implies a lower thermal mixing efficiency.

Figure 6, shows the strong dependence of thermal mixing performance on the sparger configuration and hole distribution pattern. The staggered-type spargers (Sp1, Sp3 and Sp5) have much poorer performance than the parallel-type spargers (Sp2, Sp4 and Sp6). Therefore, the effect of the hole distribution pattern should be considered. The P/D effect on thermal mixing performance can be explained by considering the relation between the interaction of neighboring steam jets and the steam discharging velocity. In summary, the thermal mixing performance as well as the characteristics of the pressure pulse, such as amplitude and frequency, need to be considered for proper design and/or selection of spargers and quench tanks.

3.2   Frequency of pressure oscillation

In the condensation oscillation mode, pressure fluctuation is characterized by a dominant frequency. In the present study, pressure oscillations in the water pool are measured at low mass fluxes between $G=70$ and 215 kg/m²-s. The pressure sensor location is shown in Fig. 1. The pressure oscillation frequency is analyzed with a fast Fourier transformation (FFT) technique (Bendat and Piersol, 1991). A typical pressure signal in the time domain is shown in Fig. 2.

Simpson et al. (1982) investigated the basic mechanism of steam condensation at a relatively low mass flux, and observed that the characteristics of unstable jets are different from those of stable jets. They suggested the relation in Eq. (3),

$$St = k_1(\mathrm{Ja})^{a1}(\mathrm{Re})^{b1} \qquad (3)$$

where Ja is the Jacob number, which is the ratio of the specific energy absorption capability of the liquid to the energy density of the steam; Re is the Reynolds number based on the nozzle diameter; and St is the density weighted Strouhal number. The constants in Eq. (3) are $k_1=0.011$, $a_1=$
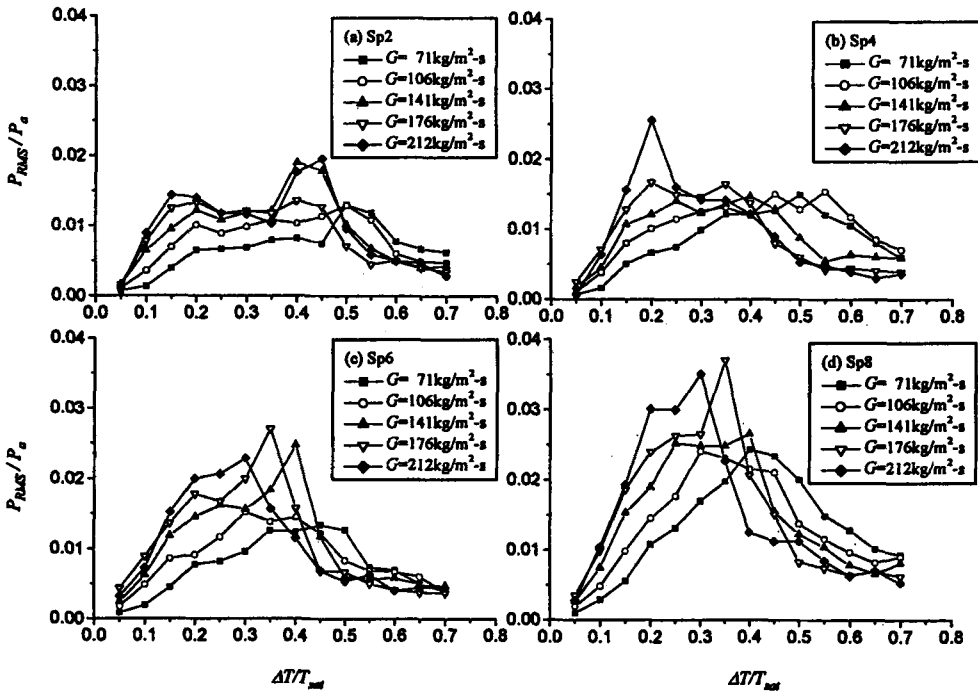
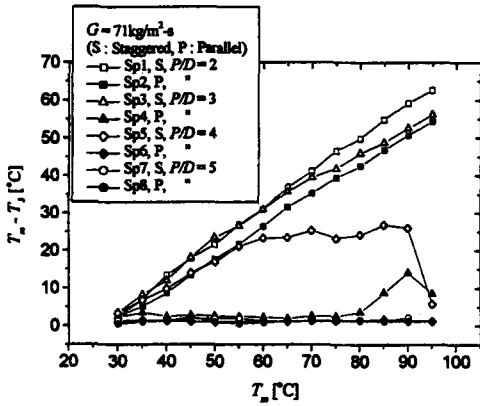Fig. 5   Variation of pressure amplitude of parallel type spargers

Fig. 6   Temperature difference between the mean value and T₃ with a variation of the sparger

0.72, and $b_1=0.25$. Damasio et al. (1985) proposed an improved correlation, which includes the Weber number to take into account the surface tension effect.

$$St = k_2(Ja)^{a2} \ (Re)^{b2} \ (We)^{c2} \qquad (4)$$

where the constants are $k_2=0.001196$, $a_2=1.0849$, $b_2=0.9389$, $c_2=-0.7670$.
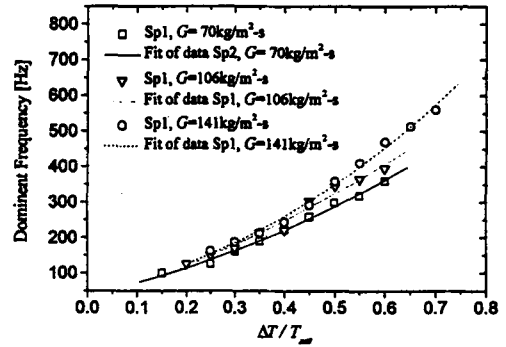

Fig. 7   Variation of the dominant frequency with the steam mass flux in the case of Sp1

In Figs. 7 and 8, the variation of the dominant frequencies vs. the degree of pool water subcooling is shown. The dominant frequency is nearly proportional to the pool water subcooling. At low pool temperatures, the discharged steam breaks up into small bubbles with fast condensation speed and short lifetime. On the other hand, as the pool temperature increases, the size and lifetime of these disintegrated bubbles increase.
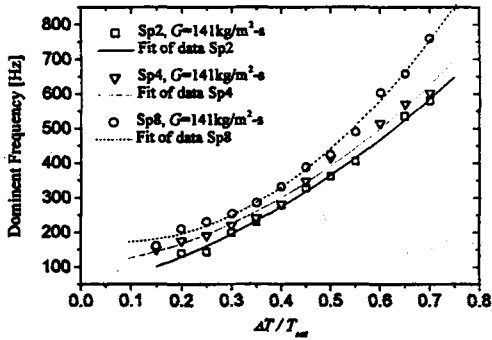
Fig. 8 Variation of the dominant frequency with the P/D ratio of the sprager

Fig. 9 Comparison of the dominant frequency with other correlations in the case of Sp8 at $G=141\mathrm{kg/m^2}$-s

Accordingly, the dominant frequency increases with increasing pool subcooling. The dominant frequency increases slightly with steam mass flux as shown in Fig. 7. Moreover, as P/D increases, the dominant frequency also increases (Fig. 8). As P/D decreases, a discharging steam jet can readily combine with neighboring ones. Thus the steam bubble becomes larger than that of a single jet. For this relatively large steam bubble, the condensation period is lengthened. Therefore, the dominant frequency decreases slightly. In summary, the geometric configuration of the spargers as well as the sparger dimensions are important factors affecting the frequency of pressure oscillation.

In Fig. 9, the experimental data of Sp8 are compared with other correlations. Damasio's correlation shows a good agreement with the present data. Since P/D of Sp8 is 5, the interaction between neighboring jets is smaller than that in others. In Fig. 10, however, the difference between the present data and Damasio's correlation becomes larger as P/D decreases. This discrepancy comes due to the interaction between neighboring jets. Therefore, sparger shape factors, hole pattern, and bore size should also be considered to correlate the frequency data from various spargers.

From the data of the present study, the following correlation is suggested:

$$St=k_3(\mathrm{Ja})^{a3}\ (\mathrm{Re})^{b3}\ (\mathrm{We})^{c3}\ (I_p)^{d3} \qquad (5)$$

The constants in Eq. (5) are $k_3=0.00174$, $a_3=1.093$, $b_3=0.891$, $c_3=-0.827$, and $d_3=0.298$, I_p is

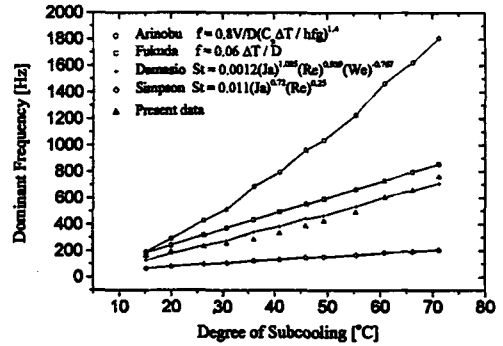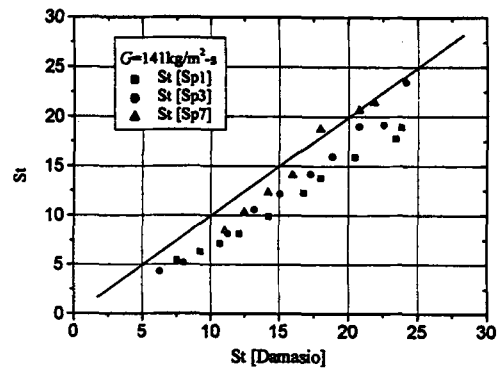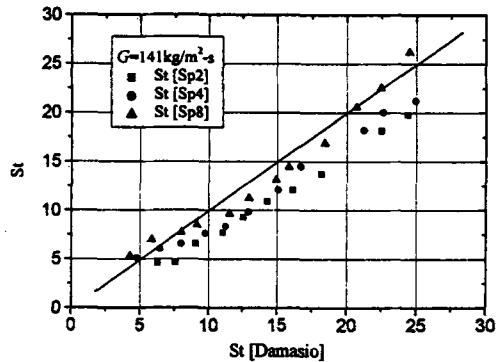(a) Staggered type

(b) Parallel type

Fig. 10 Comparison of Strouhal number with Damasio's correlation, Eq. (4)

the sparger shape factor, which corresponds to P/D. The effects of the other geometric factors are not included. A comparison of the Strouhal numbers from experiments and Eq. (5) is shown
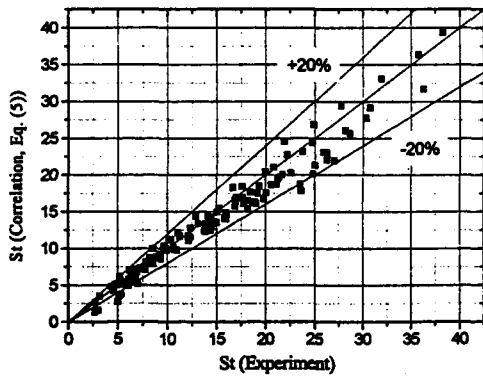
Fig. 11 Comparison of Strouhal number between the experiment and correlation, Eq. (5).

in Fig. 11. The correlation predicts the experimental data within 20%. The mechanism regarding steam bubble oscillation in water, however, has to be studied more precisely.

The dominant frequencies observed in this study are dependent on system dimensions such as the hole and the bore sizes. Therefore, more systematic studies with various sizes of spargers must be carried out.

3.3 Uncertainty analysis

The uncertainty analysis has been performed for a 95 percent confidence level. According to the ASME performance test codes 19.1 (1985), the uncertainty interval of the present results is given by the root-mean-square of a bias contribution and a precision contribution for the case of Sp8 at $G=144kg/m^2$-s. The results show that the uncertainty intervals of the dominant frequency and the amplitude of the pressure signal are 1.1 % (8.3 Hz) and 0.8 % (0.03 kPa), respectively. The uncertainty interval of the steam mass flow rate is 3.57 % of the measured value.

4. Conclusions

The pressure loads due to the direct contact condensation (DCC) of steam discharging into subcooled water have been measured for eight different spargers for various steam mass fluxes and pool water temperatures. The major parameters affecting the pressure load are the sparger configuration, the discharging hole distribution pattern, the steam mass flux, and the pool water temperature.

The major findings are summarized as follows:

(1) The amplitude of the pressure pulse shows a peak at a pool temperature of around $45 \sim 85°C$ depending on P/D and steam mass flux.

(2) The dominant frequency increases with the degree of pool subcooling and P/D. A new frequency correlation is proposed in terms of P/D and other thermal hydraulic dimensionless parameters. The dominant frequencies lie between 99 and 759Hz.

(3) The P/D ratio has a strong influence on pressure oscillation and thermal mixing. As P/D increases, the pressure pulse amplitude increases significantly.

(4) The effect of the hole distribution pattern on the dominant frequency is smaller than that of P/D.

(5) The thermal mixing performance of staggered-type spargers is much poorer than that of parallel-type sparges especially when the P/D ratio is less than 4.

In the design and/or selection of an optimal sparger related to the DCC phenomena, thermal mixing effects as well as the pressure pulse characteristics should be considered.

Acknowledgment

References

Arinobu, M, 1980, "Studies on the Dynamic Phenomena caused by Steam Condensation in Water," *Proc. of ANS-ASME-NRC Int. Topical Meeting on Nuclear Reactor Thermal Hydraulics*, Vol. 1, pp. 293~302.

Aya, I., Kobayashi, M., and Nariai, H., 1983, "Pressure and Fluid Oscillations in Vent System due to Steam Condensation, (II) High-Frequency Component of Pressure Oscillations in Vent Tubes under at Chugging and Condensation

Oscillation," *J. of Nuclear Science and Technology*, Vol. 20, No. 3, pp. 213~227.

Bendat, J. S., and Piersol, A. G., 1991, "Random Data Analysis and Measurement Procedures," *John Wiley & Sons*.

Chan, C. K., 1978, "Dynamic Pressure Pulse in Steam Jet Condensation," *Proc. of 6th Int. Heat Transfer Conf.*, Toronto, pp. 395~399.

Cho, S., Song, C.-H., Park, C.K., Yang, S.K., and Chung, M.K., 1999, "Studies on dynamic pressure oscillation induced by direct condensation of steam discharging through I-type sparger," *Proc. of the KSME thermal engineering division fall meeting*, Sorak Han Hwa resort, Korea, pp. 532~539.

Cumo, M., Farello, G.E., and Ferrari, G., 1978, "Direct Heat Transfer in Pressure-Suppression Systems," *Proc. of 6th Int. Heat Transfer Conf.*, Toronto, Vol. 5, pp. 101~106.

Damasio, C., Del Tin, G., Fiegna, G., and Malandrone, M., 1985, "Experimental Study on the Unstable Direct Contact Condensation Regimes," *Proc. Of 3rd Int. Topical Meeting on Reactor Thermal Hydraulics*, Newport, Rhode Island, U.S. A., pp. 6. C-16. C-8.

Fukuda, S, 1982, "Pressure Variations due to Vapor Condensation in Liquid, (II) - Phenomena at Larger Vapor Mass Flow Flux," *J. of Japanese Atomic Society*, Vol. 24, No. 6, pp. 466~474.

Simpson, M.E., and Chan, C.K., 1982, "Hydraulics of a Subsonic Vapor Jet in Subcooled Liquid," *ASME J. of Heat Transfer*, Vol. 104, pp. 271~278.

Sonin, A.A., 1984, "Suppression Pool Dynamics Research at MIT," NUREG/CP-0048, pp. 400~421.

The American Society of Mechanical Engineers, 1985, "Measurement Uncertainty-ASME Performance Test Codes, Supplement on Instruments and Apparatus, Part I," ANSI/ASME PTC 19. 1-1985.

Tin, G.D., Lavagno, E., and Malandrone, M., 1982, "Pressure and Temperature Measurements in a Vapor Condensing Jet," *Proc. of 7th Int. Heat Transfer Conf.*, Vol. 6, pp. 159~164.